Invited Paper

Real-time Image Processing using Photorefractive Crystals

Ken Y. Hsu, S. H. Lin
Institute of Electro-Optical Engineering
National Chiao Tung University
Hsinchu, Taiwan, R.O.C.
and
T. C. Hsieh
Department of Electro-Physics
National Chiao Tung University
Hsinchu, Taiwan, R.O.C.

ABSTRACT

We describe the combination of neural network training and volume holographic storage technologies using photorefractive crystals for real-time image processing. Experimental results on using the system for multi-channel distortion-invariant image recognition are presented.

1. Introduction

In recent years photorefractive (PR) crystals have been extensively studied for their applications in optical computing. In general, there are two different types of applications to use these media. One application is the mass data storage by using the volume hologram. Five thousand images have been successfully stored in a Fe:$LiNbO_3$ crystal using the angular multiplexing technique [1]. In principle, the storage density of the crystal volume can be up to 10^{12} bits/cm^3. Furthermore, by storing the holographic matched filters at different reference angles, a multi-channel image correlation system has been proposed [2]. The second application of the photorefractive crystals is to use the material as the dynamical recording medium for real-time information processing such as the optical wave-mixing, optical phase conjugation, optical interconnection, and especially the optical neural networks. In this application, information is stored as the amplitudes of the holographic gratings in photorefractive crystals. The shape and amplitude of the gratings can be modified in real-time. The response time is in the range from micro-seconds to several seconds, depending on the materials and the light intensities. The advantage of this type of information processing is that very large number of interconnections can

 0-8194-1778-5/94/$6.00

be stored, retrieved, processed, and modified in parallel. Several architectures have been proposed and some hardware implementation have demonstrated. [3-5] In this paper, we present the combination of these two types of technology for real-time image recognition. In section 2, we describe the technique of holographic storage in a 45^0-cut iron-doped lithium niobate crystal. By using the crystal for recording the holographic matched filters, a multi-channel image correlation system is presented. In section 3, a heavily doped Fe:$LiNbO_3$ crystal plate (0.6 % mole iron concentration, 50 μm thick) is used as the dynamical holographic media for the implementation of the optical inner product. A hybrid neural network which combines the optical inner product and a personal computer is assembled to implement the perceptron learning algorithm. Experimental results on using the system for real-time pattern classification are presented. In section 4, the hybrid network is combined with the holographic storage system to form a multi-channel neural network. The system performs the multi-category pattern recognition. Experimental results are presented. Finally, in section 5, the paper conclusions are presented.

2. Multi-channel correlator by volume hologram

Angular-multiplexing technique is one of the most commonly used schemes of storing multiple holograms in a holographic volume. With this type of data storage, parallel and fast read-out of information can be accomplished simply by changing the incident angle of the reference beam. Five thousand holograms have been successfully recorded in a Fe:$LiNbO_3$ crystal. In this type of information storage, if the crystal is set at the filter position of the Vander Lught correlator, then each hologram is a matched filter, and the multi-channel correlation can be achieved.

In this paper, a multi-channel correlator using volume holographic technique has been constructed. The architecture of the system is shown in Fig.1. A collimated laser beam from an argon laser (λ = 514 nm) passes through a liquid crystal television (LCTV, LQ-1000 produced by Sharp) for carrying the input information. The resolution of the LCTV is 400 x 380 pixels with a panel dimension of 6 x 4 cm^2. This size is larger than the clear aperture of our optical components, hence only half of the panel is used for displaying the input images. After the LCTV, lens L1 (focal length = 40 cm) produces the Fourier transform of the input pattern at the filter plane P2. Then, lens L2 (focal length = 16 cm) images the Fourier spectrum from P2 plane onto the photorefractive crystal at plane P3. An iron-doped $LiNbO_3$ crystal is used for storing the multiple holograms of the matched filters. To achieve the angular-multiplexing multiple storage, each hologram is recorded with the reference beam incident at different angles. The reference beam is derived from an argon laser by beam splitter BS, mirror M1, and lenses L4, and L5. Mirror M1, lenses L4 and L5 form a telescope 4-f system which is focused at infinity. Mirror

M1 is mounted on a rotation stage and its center is at one focal point of the telescope, and the crystal is at the other focal point. Hence, the position of the reference beam on the crystal remains unchanged when the incident angle of the reference beam is adjusted by tuning either the horizontal or the vertical gimbals of M1.

Note that in the system, the pixelized structure of LCTV produces many orders of diffraction of the Fourier spectra. In order to select one of the diffraction orders, we place a band-pass spatial filter at P2 plane. This filter also blocks the dc spot of the Fourier spectrum. It produces the edge enhancement effect to the input pattern. Fig. 2 shows examples of the input patterns and their edge enhancement versions. Another point is that, the geometrical scheme for the storage is the θ=90° configuration, where θ is the angle between the reference beam and the bisector of the object beam. The optical axis of the crystal is along the direction of the grating vector. This set-up minimizes the angular separation requirement of the angular-multiplexing at the same time provides the maximum diffraction efficiency. [6]

After the holographic matched filters are recorded, the reference beam is blocked off, and the images to be recognized are presented on the LCTV for the correlation operation. The diffracted signal from the crystal is Fourier transformed by lens L3 (focal length = 10 cm) onto the correlation plane. The output signal is detected by a two dimensional detector array, in our case it is a CCD camera. The mathematical operation of this multi-channel correlation can be written as :

$$g(x_4,y_4)=\sum_{m,n} f\otimes h_{mn}(x_4,y_4)*\delta(x_4-m\Delta x,y_4-n\Delta y) \qquad (1)$$

where $\otimes$ is the correlation operation, $*$ is the convolution operation, f(x,y) is the input function, $h_{mn}(x,y)$ is the filter function corresponding to the matched filter at different reference angles, and the δ-function means that the centers of the correlation would be at different positions which depends on the recording angles of the reference beams. If the focal length of lens L3 is L and the angles of separation for the neighboring exposures in horizontal and vertical axes are $\Delta\theta_x$ and $\Delta\theta_y$, respectively, then Δx and Δy are written as:

$$\Delta x = L\cdot\Delta\theta_x, \quad \Delta y = L\cdot\Delta\theta_y \qquad (2)$$

Fig. 3 shows the experimental results. In the experiment, fifty filters are recorded in the crystal and each filter corresponds to a Chinese signature. Figures 3(a) and 3(b) show that when one of the signatures is input into the system, the correlation peak appears at the corresponding position. Fig. 3(c) shows that when the input is a rotated version of the input of Fig. 3(a), the original correlation peak disappears. Instead, it is recognized as another pattern and the correlation peak appears at the other position if the matched filter for this rotated pattern is recorded at a different reference angle in the crystal. Furthermore, Fig. 3(d) shows that when part of the input pattern is similar to that of Fig. 3(c), then it produces two correlation peaks. These results show that the optical correlator can not tolerate either rotation or distortion of the input images. In next section, we will present an optical neural network to resolve this problem.

3. Pattern recognition based on hybrid perceptron learning

The synthesis of a matched filter which has the capability of distortion tolerant image recognition has been an interesting subject to the researchers in optical information processing.[7] Recently, a neural network approach has been proposed and demonstrated.[8-9] In that approach, the dynamic characteristics of PR crystals has been used for implementing the learning behavior of neural networks. After the training, the weights of interconnections can be used for distortion-tolerant image recognition. However, it was discussed in [10] and [11] that the finite response time and hologram erasure characteristics of the photorefractive gratings impose constraints on the convergence property of the perceptron learning. And it was proposed in [12] that a hybrid method for implementing the perceptron learning algorithm could resolve the convergence problem. Thus, the hybrid perceptron learning will be used in this paper and is reviewed in this section.

The goal of the perceptron network is to classify a set of training patterns $\{\underline{x}_1, \underline{x}_2, \cdots\cdots, \underline{x}_M\}$ into two groups which are specified as class C1 or C2, depending on whether the value of the inner product $\underline{w}\,\underline{x}$ is higher or lower than the threshold value θ, where $\underline{w}$ is the interconnection weight vector and is obtained through learning. The perceptron learning rule is written as :

$$\underline{w}(k+1) = \underline{w}(k) + \alpha(k) \cdot \underline{x}(k) \qquad (3)$$

where $\underline{x}(k)$ is the k-th input vector, $\alpha(k)$ is the updating factor, and k is the integer registering the number of interrogation. The updating factor is obtained according to the following rule:

$$\alpha(p)=\begin{cases} 0 & \text{if } \underline{x}(p) \text{ is correctly classified} \\ 1 & \text{if } \underline{x}(p)\in C1 \text{ , but } \underline{w}(p)\cdot\underline{x}(p)<\theta \\ -1 & \text{if } \underline{x}(p)\in C2 \text{ , but } \underline{w}(p)\cdot\underline{x}(p)>\theta \end{cases} \tag{4}$$

where the θ is the threshold value and C1 (or C2) represents the category of the patterns whose output value is 1 (or -1).

It is seen from Eqs. (3) and (4) that, in order to implement the perceptron learning algorithm, there are three operations to be performed: 1). updating of the weights, 2). memorizing the interconnection weights, 3). inner product operation of $\underline{w}\cdot\underline{x}$ and thresholding. In our system, the first two operation are performed by a personal computer, and the third operation is achieved by the optics. The schematic diagram for the complete system is shown in Fig. 4. It consists of two parts : an optical unit plus a personal computer. The optical part is a structure similar to an optical joint-transform correlator.[13] A photodetector is placed at the central position of the correlation plane. It was shown that this arrangement performs the inner product operation. [14] On the other hand, the personal computer is used to program and control the training procedure. The advantage of the hybrid system is combination of the programmability of the digital computer and the parallel computing property of optical systems. In addition, since the interconnection is stored in the computer, it is a non-volatile memory and could be used for post-processing.

Now we describe the training procedure. The training patterns $\underline{x}$ and the initial value of the interconnection weight $\underline{w}(0)$ are stored in the personal computer. Then the pattern $\underline{x}$ is sent to one arm of the network through one half of LCTV screen and the weight $\underline{w}$ is presented to the other half of the LCTV. Lens L1 (focal length = 40 cm) produces the joint transformation of $\underline{x}$ and $\underline{w}$. A Fe:$LiNbO_3$ crystal plate is set at the Fourier plane of L1 to record the interference fringes of the joint transformation. The thickness of the crystal plate and the incident angles of the writing beams are arranged such that the photorefractive gratings satisfy the condition of thin holograms. [15] A He-Ne laser beam is incident from the back side of the crystal plate to read out the interference gratings. The diffracted signal is Fourier transformed by lens L2 and detected by a photodetector. The signal is sent to the computer for the thresholding operation. The result is compared with the specified value (class) of the input pattern to generate the updating signal. Using the updating signal in Eq. (3), $\underline{w}(k)$is updated by either adding to it or subtracting from it the pattern $\underline{x}(k)$. The addition and subtraction are performed in the personal computer and the updated $\underline{w}(k+1)$ are stored in the computer memory. The iterations continues until all the patterns are correctly classified.

In the perceptron operation, we consider the case that $\underline{x}$ are patterns with either zero or positive elements, whereas $\underline{w}$ can be bipolar because it is the linear combination of $\underline{x}$. In our experiments, the LCTV is operated in amplitude modulation mode and only unipolar patterns with 0-255 gray levels can be displayed. To resolve this problem, the bipolar $\underline{w}$ is split into two positive unipolar patterns:

$$\underline{w} = \underline{w}^{+} - \underline{w}^{-} \tag{5}$$

where $\underline{w}^{+}$ is the vector of which its non-zero elements are equal to the corresponding positive elements of $\underline{w}$, and other elements of $\underline{w}^{+}$ are zero which corresponds to the negative and zero elements of $\underline{w}$. Similarly, $\underline{w}^{-}$ has non-zero elements which has the magnitude of the corresponding negative element of $\underline{w}$, and it has zero elements at the positive and zero elements of $\underline{w}$. Then, each inner product can be obtained in two steps. In the first step, $\underline{w}^{+}$ and $\underline{x}$ are presented on the LCTV and $\underline{w}^{+}\cdot\underline{x}$ is detected by the optical detector. In the second step, $\underline{w}^{-}$ and $\underline{x}$ are displayed and $\underline{w}^{-}\cdot\underline{x}$ is detected. Then the two signals are subtracted in the personal computer. Since

$$\begin{aligned} \underline{w}^{+}\cdot\underline{x} - \underline{w}^{-}\cdot\underline{x} &= \left(\underline{w}^{+} - \underline{w}^{-}\right)\cdot\underline{x} \\ &= \underline{w}\cdot\underline{x} \end{aligned} \tag{6}$$

hence the inner product $\underline{w}\cdot\underline{x}$ is obtained.

Fig. 5 shows the training patterns, of which the handwritten Chinese character and its scale-, rotated-versions and the identical characters written by the second person are specified as class C1. Some other characters are specified as class C2. Fig. 6 shows the training curve. The threshold value of the network is set as 0. It is seen that the patterns are correctly classified after three cycles of iterations, where one cycle means the check of all the patterns in the training set. We then use the solution $\underline{w}$ for image recognition. These eight patterns and the interconnection weight $\underline{w}$ are presented into the optical system and the inner products are detected. Fig. 7 shows the experimental results. It can be seen that the C1 patterns produce high inner product values and the C2 patterns produce low values. They are correctly recognized.

4. Multi-category distortion-invariant pattern recognition

It was demonstrated in section 2 that a multi-channel image correlation system can be achieved by storing the holographic matched filters at different reference angles. Using the same multiplexing technique, the two-category image recognition system described in the section 3 can be extended to a multi-category case. To achieve this, the interconnection weight vector for each image is firstly obtained through the hybrid perceptron learning. Each weight vector is stored in the computer. Then each vector is recorded as a holographic filter in the photorefractive crystal at different reference angles. And this volume hologram is the optical filter for multi-channel distortion-invariant image recognition. Figure 8 shows the schematic diagram for the complete system. In the figure the block inside the dashed line is the part for the perceptron learning. After the training, the interconnection weight vectors are displayed on the LCTV and recorded as holographic filters in the Fe:$LiNbO_3$ crystal. Filters for $\underline{w}^+$ and $\underline{w}^-$ of each image are recorded as one neighboring pair in the volume hologram. The diffracted signals from the filter pair are detected and subtracted in the computer. Thus the operation in Eq.(6) is realized in one step.

After the multi-channel filters are recorded, the system is ready for image recognition operations. When an input image is displayed at the position of $\underline{w}$ on the LCTV, the output of the multi-channel inner product is detected by the linear array of photo detectors. The signal is sent to the computer to produce the array of the recognition signal. The position of the peak signal indicates which image is recognized. In our experiment, the system is assembled to recognize ten handwritten Chinese characters. Therefore, there are twenty filters required, ten for $\underline{w}^+$ and the other ten for $\underline{w}^-$. These twenty filters are recorded in the crystal. For image recognition, when the input is belong to class $\underline{x}_4$, a peak signal is obtained at the fourth position of the output array. On the other hand, when the input is belong to class $\underline{x}_8$, a high signal is obtained at the eighth position of the output array.

The experimental results are shown in table 1. The table shows two columns of recognition results for the purpose of comparisons between the trained- and untrained-network. In the table 1(a), the input are the rotated versions of a Chinese character. In the trained case, both are recognized as class $\underline{x}_4$. In the untrained case, which is the output of an optical correlator described in section 2, the correlation signal disappears as the input is rotated. Hence, an additional filter for the rotated version must be recorded at a different reference angle, and the rotated image is recognized as a different image at position 9. Similarly, in table 1(b), both the distorted versions of the Chinese character are recognized by the trained network as $\underline{x}_8$. Whereas in the untrained case, the two versions are recognized as two distinct patterns at the positions 4 and 6, respectively.

5. Conclusion

We have presented and demonstrated an image recognition system which has combined the learning capability of neural networks and the multi-channel storage characteristics of the volume holography. A hybrid perceptron learning network is used in this paper. It provides the advantages of parallelism of optics and the programmability of electronics. In addition, a Fe:$LiNbO_3$ crystal is used for the angular multiplexing recording of multi-channel holographic filters. The filters perform the multi-channel inner product in parallel. And the system has performed a distortion-invariant multi-channel image recognition.

6. Acknowledgment

This research is supported by the National Science Council, Taiwan, R.O.C. under contract NSC 83-0416-E-009-012.

7. REFERENCES

1. F. H. Mok, "Angle-multiplexed storage of 5,000 holograms in lithium niobate", *Opt. Lett.*, **18**, No.11, 915-917 (1993).
2. F. H. Mok and H.M. Stoll, "Holographic inner-product processor for pattern recognition", *Proc. SPIE,* **1701** (1992).
3. D. Psaltis, D. Brady and K. Wagner, "Adaptive optical networks using photorefractive crystals", *Appl. Opt.*, **27**, 1752-1759 (1988).
4. E.G. Paek, J.Wullert and J.S. Patel, "Holographic implementation of a learning-machine based on a multicategory perceptron algorithm", *Opt.Lett.*, **14**, 1303-1305 (1989).
5. J. Hong, S. Campbell and P. Yeh, "Optical pattern classifier with perceptron learning", *Appl. Opt.*, **29**, 3019-3025 (1990).
6. F.T.S Yu, *Optical Signal Processing, Computing, and Neural Networks.*, JOHN WILEY & SONS, New York, 255-262, 1992.
7. F.T.S. Yu, X. Li, E. C. Tam, S. Jutamulia, and D.A. Gregory, "Detection of Rotational and Scale Varying Objects with a Programmable Joint Transform Correlator", *Proc. SPIE*, 1053, 253 (1989).
8. K.Y. Hsu, H.Y. Li and D. Psaltis, "Optical implementation of a fully connected neural network", *Proc. IEEE*, **78**, 1637-1645 (1990).

9. K.Y. Hsu, S.H. Lin, C.J. Cheng, T.C. Hsieh and P. Yeh, "An optical neural network for pattern recognition", *Int. J. Opt. Comput.* **2**, 409-423 (1991).
10. K.Y. Hsu, S.H. Lin and P. Yeh, "Conditional convergence of photorefractive perceptron learning", *Opt. Lett.*, **18**, 2135-2137 (1993).
11. C.J. Cheng, P. Yeh and K.Y. Hsu, "Generalized perceptron learning rule and its implications for photorefractive neural networks", To appear in *J. Opt. Soc. Am.* B, **11**, No.9 (1994).
12. K.Y. Hsu, S.H. Lin and T.C. Hsieh, "A hybrid neural network for image classification", submitted to *Lasers and Optics in Engineering*, August, 1994.
13. F.T.S. Yu and X.J. Lu, "A real-time programmable joint transform correlator", *Opt. Comm.*, **52**, No.1, 10-16 (1984).
14. K. Hsu, S.H. Lin, and T.C. Hsieh, "Photorefractive crystals for real-time image processing", *Proc. SPIE*, Vol. CR48, San Diego, July, 1993.
15. A. Yariv and P. Yeh: Optical *Waves in Crystals*, Wiely Interscience, New York, (1983), p. 358.

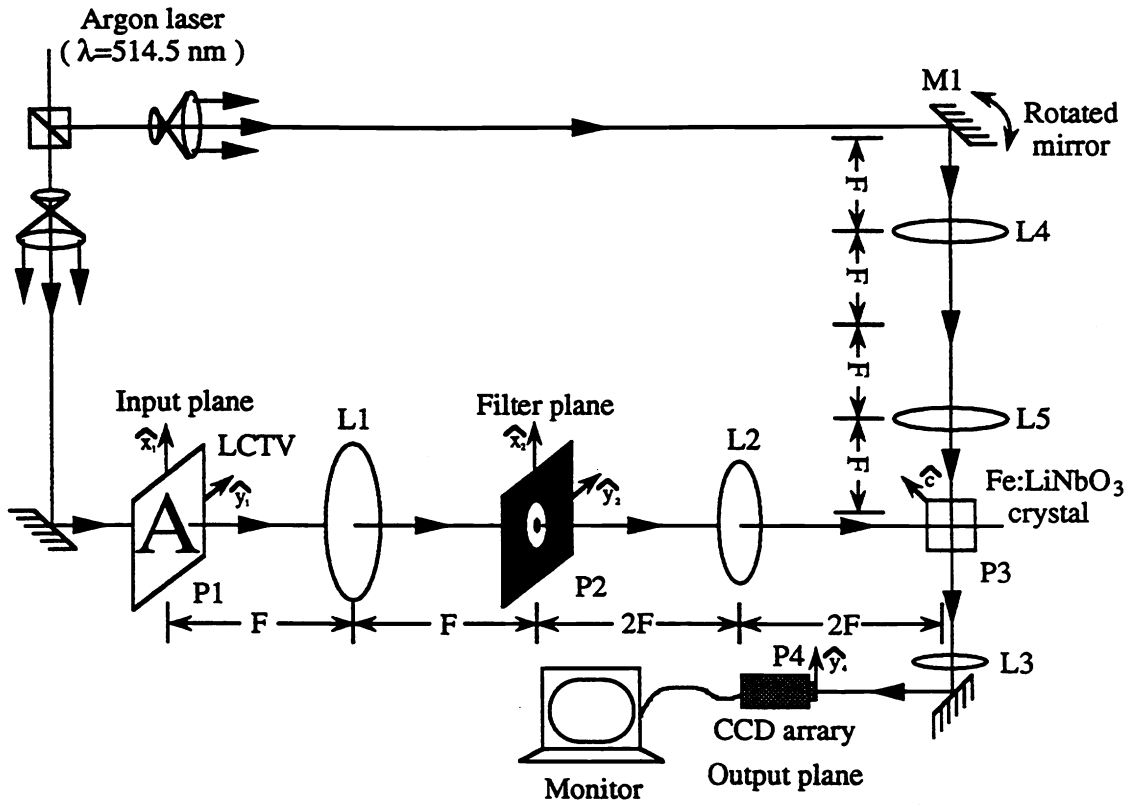

Fig. 1 The schematic diagram for the multi-channel optical correlator system.

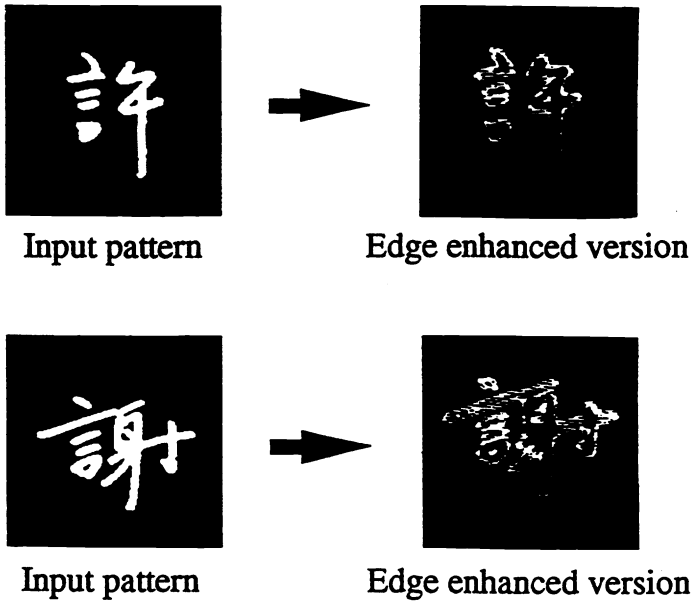

Fig. 2 The input patterns and their edge enhancement version.

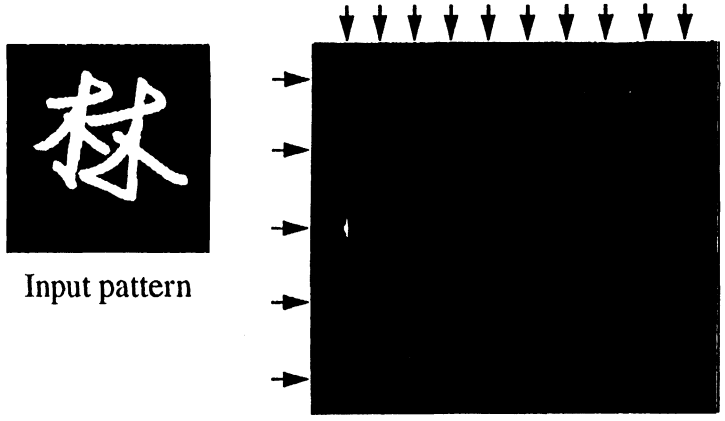

Fig.3(a) Output of character "Lin"

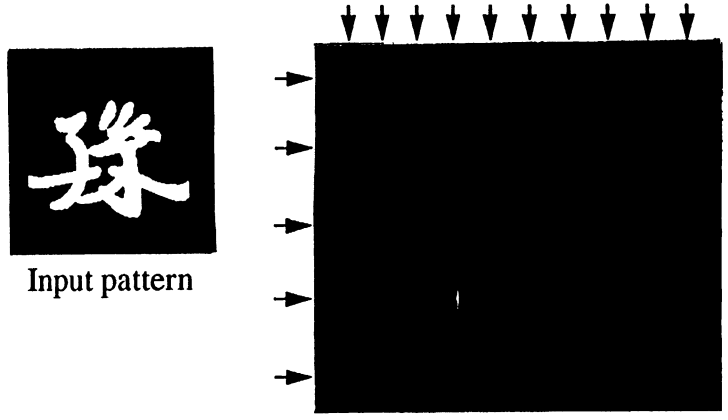

Fig.3(b) Output of character "Shun"

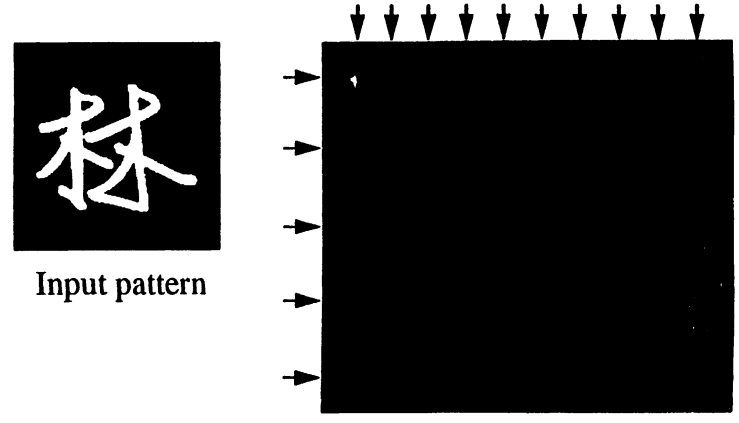

Fig.3(c) Output of rotated version of character "Lin"

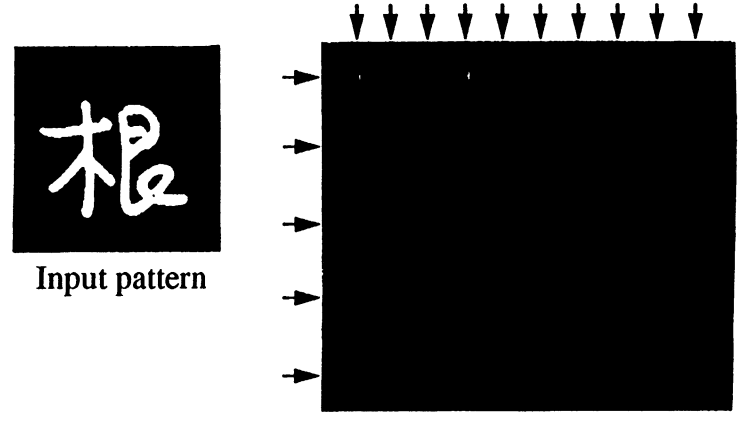

Fig.3(d) Output of character "Ken", it is similar to "Lin"

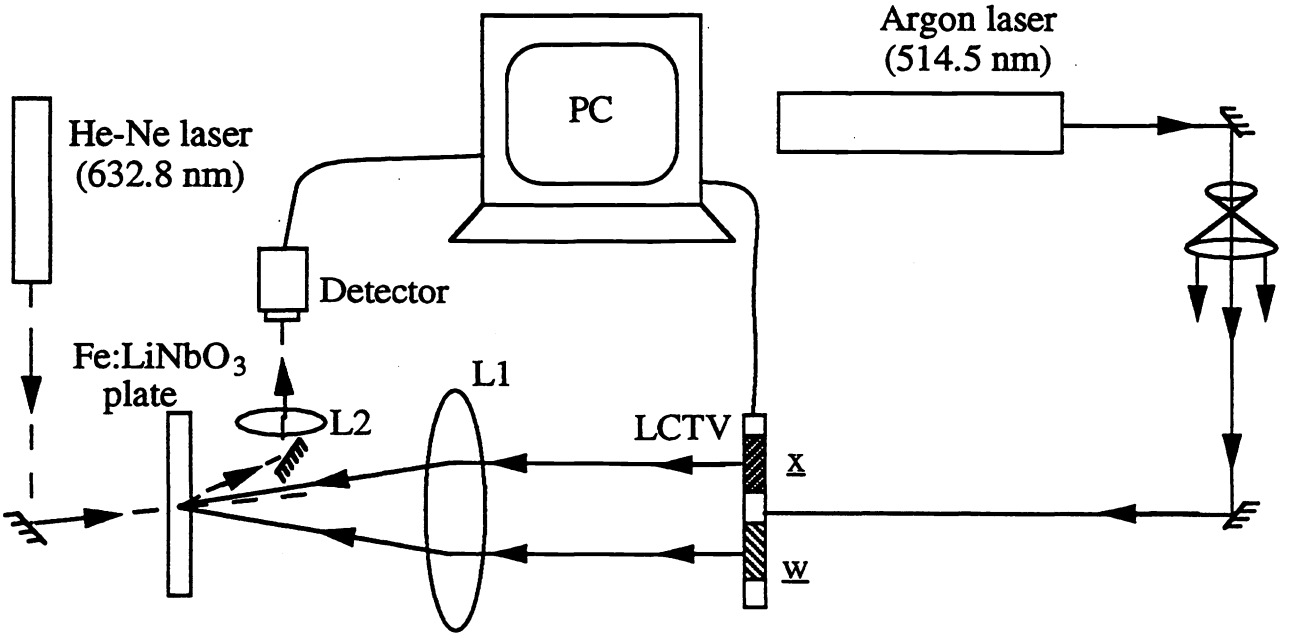

Fig. 4 The schematic diagram for the hybrid perceptron system.

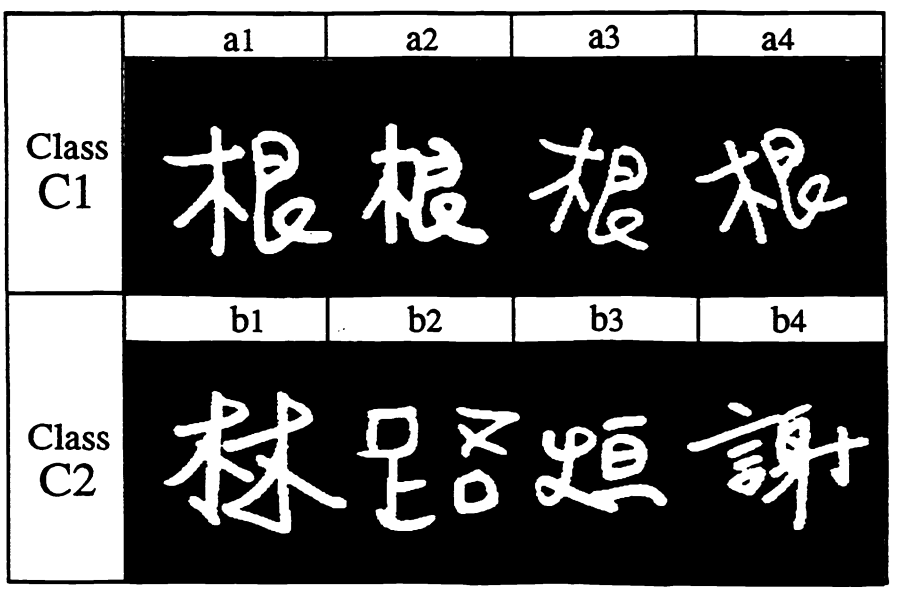

Fig. 5 The training patterns.

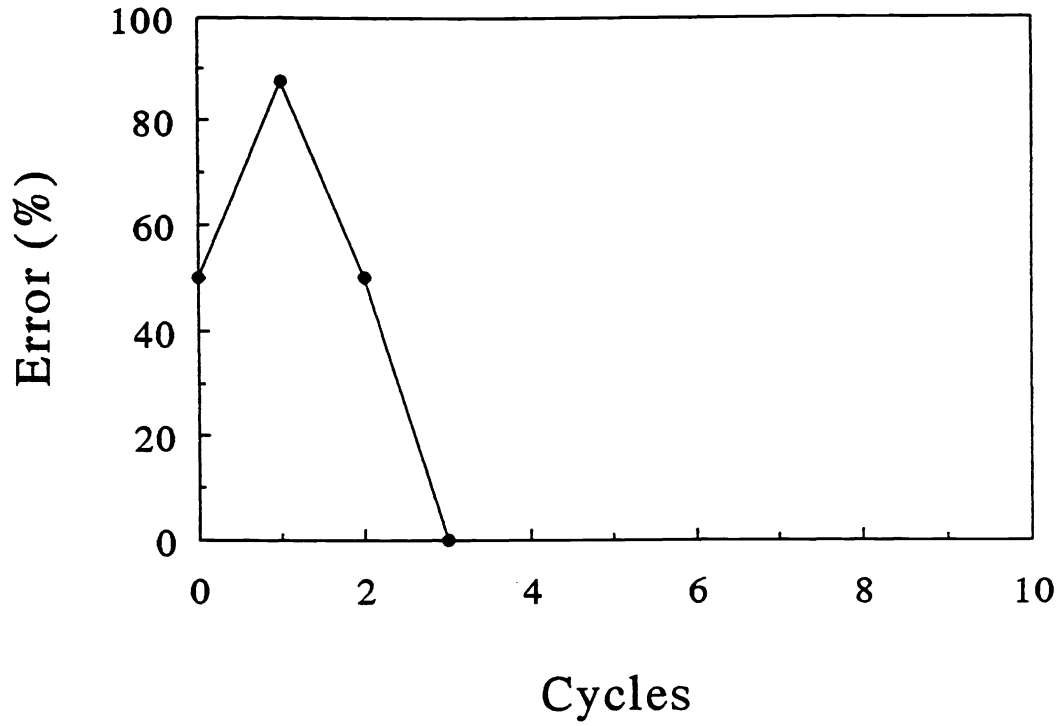

Fig. 6 The learning curve.

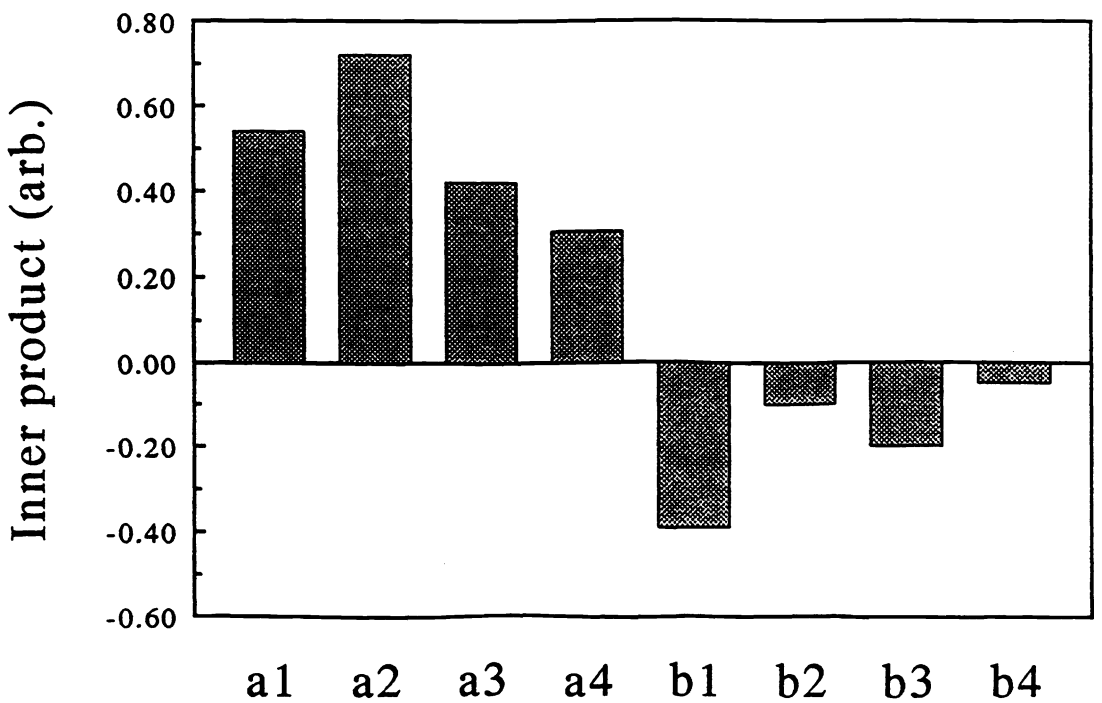

Fig. 7 The experimental result of the image recognitions.

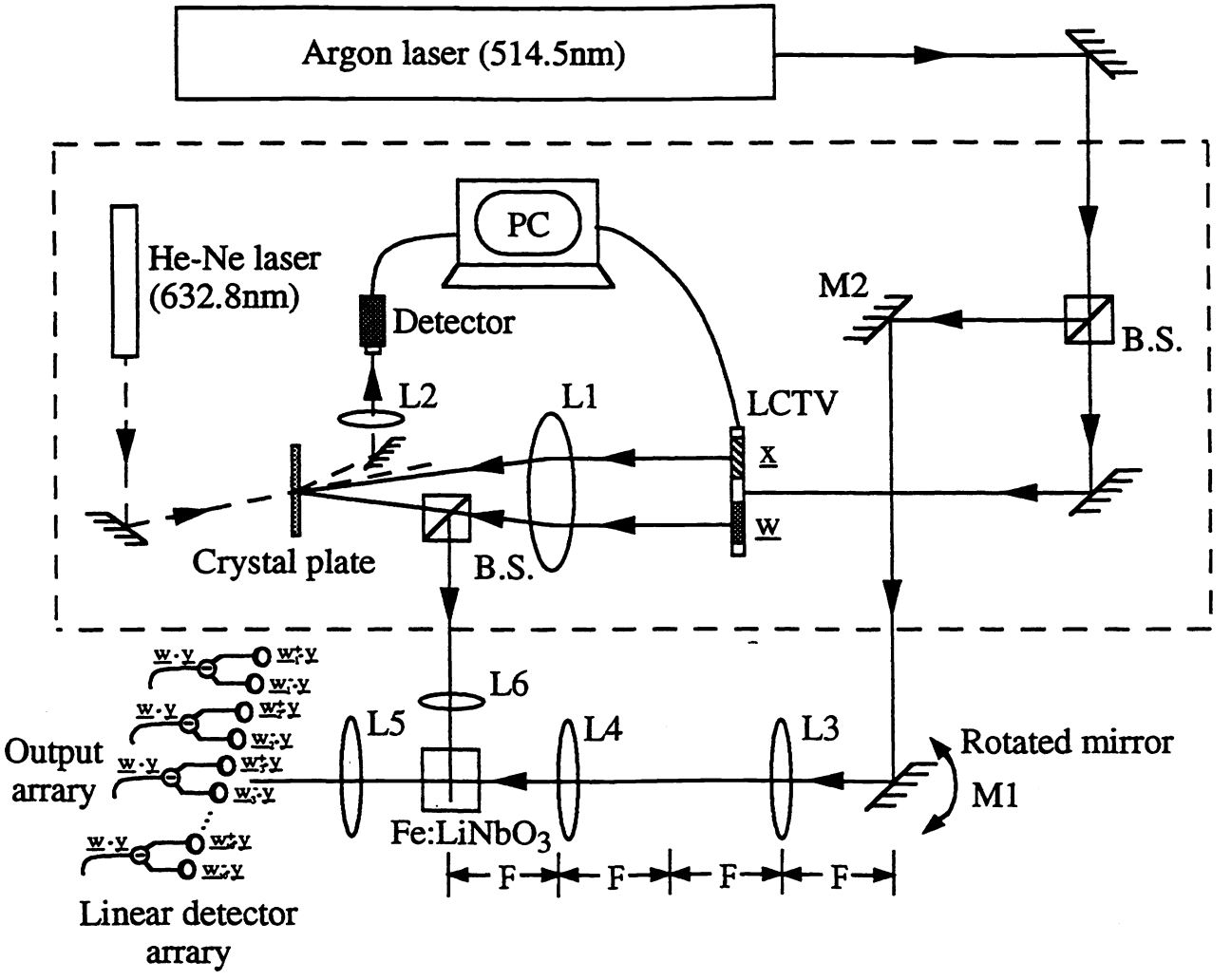

Fig. 8 The schematic diagram of the multi-category image recognition system.

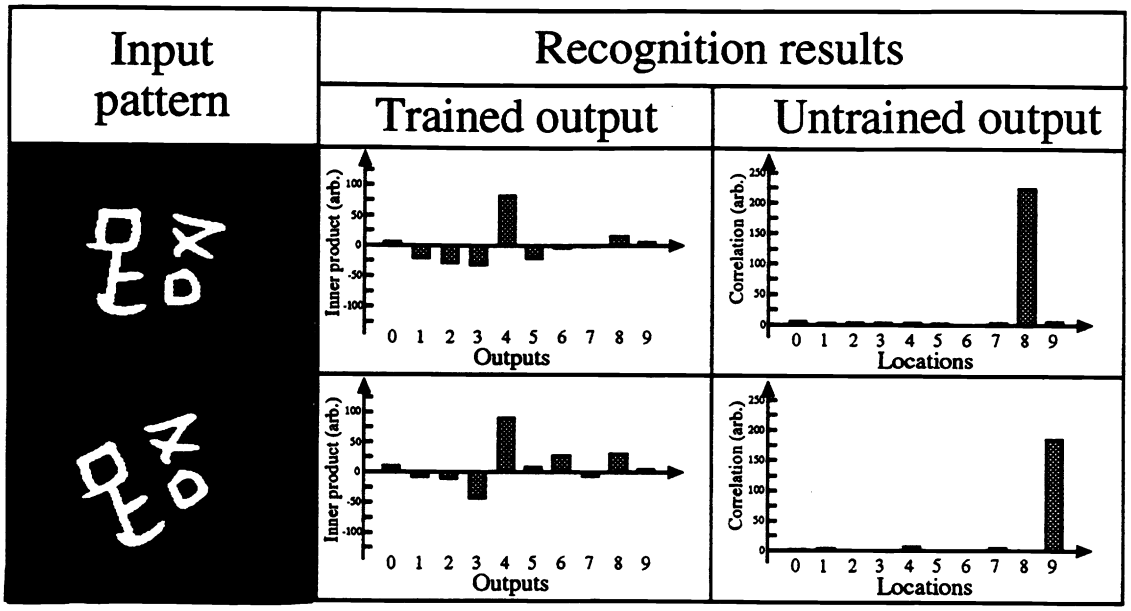

Table 1(a) The recognition results of the rotated images

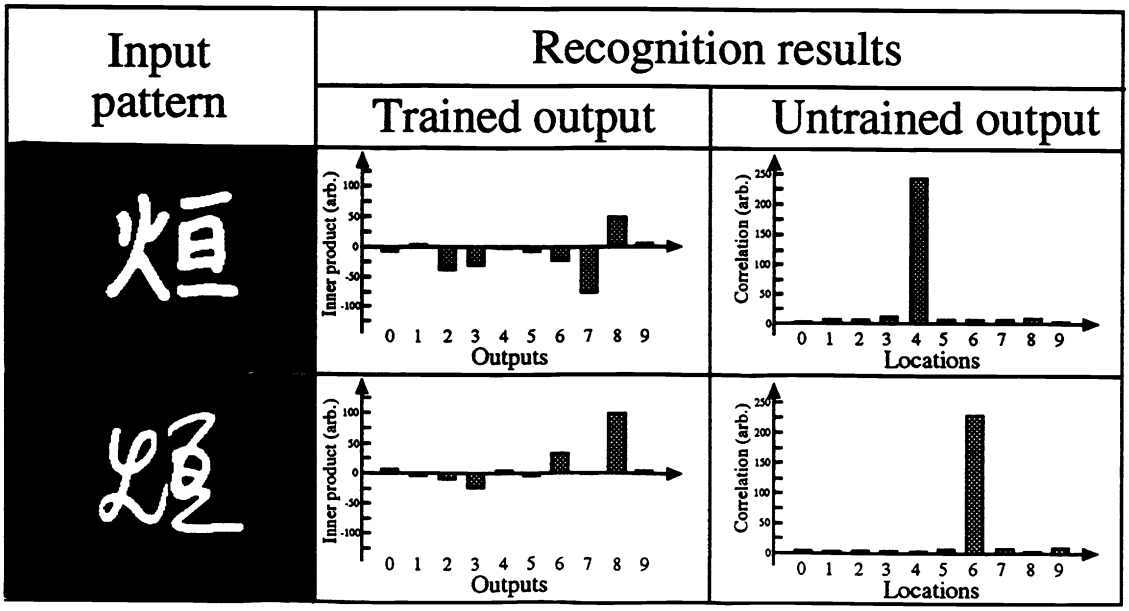

Table 1(b) The recognition results of the distorted images